Emission Quenching Mechanisms in *Octopus vulgaris* Hemocyanin: Steady-State and Time-Resolved Fluorescence Studies†

Fernanda Ricchelli,*,‡ Mariano Beltramini,§ Lucia Flamigni,∥ and Benedetto Salvato‡,§

Department of Biology, CNR Center for the Physiology and Biochemistry of Hemocyanins and Other Metalloproteins, I-35131 Padova, Italy, Department of Biology, University of Padova, I-35131 Padova, Italy, and FRAE-CNR Institute, I-40126 Bologna, Italy

Received December 31, 1986; Revised Manuscript Received April 10, 1987

ABSTRACT: Fluorescence emission properties of various derivatives of *Octopus vulgaris* hemocyanin, namely, oxy, deoxy, met, half-met, half-apo, and apo derivatives, are studied by means of time-resolved and quenching techniques. Fluorescence decay can be satisfactorily fitted by two-exponential analysis in all hemocyanin derivatives. Fluorescence quenching experiments, using acrylamide, iodide, and a combination of the two, are carried out in order to correlate the observed lifetimes with different classes of fluorophores, distinguishable by their accessibility to the external quenchers. Fluorescence lifetimes of 1.2, 2.1, and 5.5 ns are attributed to buried, partially exposed, and fully exposed tryptophans, respectively, in 11S hemocyanin at pH 8.5. For 50S hemocyanin, the lifetime pattern is very similar, but a shortening of all lifetime values is observed. The fluorescence of the class of partially exposed tryptophans, situated in close proximity to the active site, is totally quenched in oxy-, met-, and half-methemocyanin. Our results rule out a Förster-type energy-transfer process from excited tryptophans to the copper–peroxide complex as a major quenching mechanism accounting for the lower quantum yield of oxyhemocyanin as compared to the deoxy and apo forms. "Heavy atom" and "paramagnetic ion" effects, due to the bound copper, fully explain the observed finding. Thus, the application of Förster's theory to calculate the tryptophan active site average distance in oxyhemocyanin is not justified. Plausible values (r = 1.5 nm) are obtained by applying Förster's theory to the complexes of hemocyanin with carbon monoxide or 1-anilino-8-naphthalenesulfonate.

Hemocyanins (Hc)[1] are multimeric copper proteins of high molecular weight [(4.5–90) × 10^5] that function as oxygen carriers in the hemolymph of several invertebrate species belonging to Mollusca and Arthropoda (Ellerton et al., 1983). In the active site the oxygen is bound as a peroxide bridge between two Cu(II) ions. The $Cu^{II}_2O_2^{2-}$ complex is the chromophoric group responsible for the intense band with a maximum at ca. 340 nm ($\epsilon \sim 20\,000$ M^{-1} cm^{-1} per binuclear active site) and a broader feature at approximately 570 nm ($\epsilon \sim 1000$ M^{-1} cm^{-1} per binuclear copper site). In the deoxy form the metal is present as Cu(I) (Brown et al., 1980) and the protein is devoid of spectral features at $\lambda > 300$ nm. The two copper ions, though bound to the same ligands (Brown et al., 1980), are not equivalent with respect to many chemical reactions (Cox & Elliott, 1974; Symons & Petersen, 1978). Furthermore, they are removed sequentially from the active site by cyanide (Salvato & Zatta, 1977; Himmelwright et al., 1980; Beltramini et al., 1984b,c). This allows the preparation of a number of derivatives: under controlled conditions, a single copper ion can be selectively removed, leading to a half-apo form (Himmelwright et al., 1980; Beltramini et al., 1984a, 1986). Also metal oxidation can be conveniently driven in order to obtain partially or fully oxidized active site derivatives (Himmelwright et al., 1980; Salvato et al., 1986a,b).

As for the fluorescence properties, Hc, although containing phenylalanine (Phe), tyrosine (Tyr), and tryptophan (Trp) residues, shows emission spectra dominated by tryptophan (Shaklai & Daniel, 1970; Klarman et al., 1977; Ricchelli et al., 1980). The emission quantum yields (Q) increase as follows: $Q_{\text{apo-Hc}} > Q_{\text{deoxy-Hc}} > Q_{\text{oxy-Hc}}$ (Shaklai & Daniel, 1970; Bannister & Wood, 1971; Klarman et al., 1977; Ma et al., 1977; Ricchelli et al., 1980). The fluorescence quenching observed upon binding of copper to apo-Hc can be attributed to a "heavy atom" effect, exclusively due to the copper ion first removed from the active site by cyanide (Ricchelli et al., 1983; Beltramini et al., 1984a, 1986).

The further fluorescence quenching observed upon binding of oxygen has been attributed by Shaklai and Daniel (1970) and Ma et al. (1970) to an efficient Förster-type radiationless energy-transfer process from the Trp excited singlet state to the copper peroxide complex. This hypothesis is based on the presence of a strong spectral overlap between the Trp emission spectrum (300–380 nm) and the absorption band in the 320–380-nm region, as well as the proximity of some Trp residues to the active site (Jori et al., 1981; Yokota et al., 1983; Linzen et al., 1985). On these bases, average Trp active site distances of approximately 2.5 and 2.1 nm, respectively, in *Levantina* (Mollusca) and *Limulus* (Arthropoda) Hc have been calculated (Shaklai & Daniel, 1970; Ma et al., 1977).

In multitryptophan proteins these measurements are performed under the assumption that each fluorophore contributes equally to the overall fluorescence emission. In Hc, however, some observations are not consistent with this assumption. Fluorescence quenching experiments on the minimal subunit (M_r 50 000) of *Octopus* Hc, (Ricchelli & Zatta, 1985; Ric-

† This work was partly supported by CNR Grant Contract 85.00383.02.

* Author to whom correspondence should be addressed.

‡ CNR Center for the Physiology and Biochemistry of Hemocyanins and Other Metalloproteins.

§ University of Padova.

∥ FRAE-CNR Institute.

[1] Abbreviations: Hc, hemocyanin; ANS, 1-anilino-8-naphthalenesulfonate Mg^{2+} salt; EDTA, ethylenediaminetetraacetate Na^+ salt; Tris-HCl, tris(hydroxymethyl)aminomethane hydrochloride.

0006-2960/87/0426-6933$01.50/0

chelli et al., 1986) showed distribution of the Trp into at least three classes, each contributing quite differently to the total fluorescence. A class of fully quencher-accessible Trp is responsible for about 35–45% of the overall emission; a further 40–45% of fluorescence is attributable to a second class of partially accessible Trp, and a third class of deeply buried Trp contributes about 10–20%. It is expected that binding of copper and oxygen does not affect homogeneously the fluorescence properties of Hc. Indeed, the fluorescence of the partially quencher-accessible Trp, postulated to be in close proximity to the active site, has been demonstrated to be "selectively and completely" quenched in oxy-Hc (Shaklai et al., 1978; Ricchelli et al., 1980, 1986).

On the basis of the above considerations, doubts as to the validity of applying Förster's theory to these systems must be considered: as the Hc fluorescence emission largely arises from the class of Trp very close to the active site, a Trp active site distance greater than 2 nm is unlikely.

With the aim to better understand the quenching mechanisms of Trp fluorescence in Hc, steady-state and time-resolved fluorescence techniques have been applied to *Octopus vulgaris* Hc in the 49S (M_r 2.7×10^6) and 11S (M_r 2.5×10^5) (Salvato et al., 1979) aggregation states. Experiments have been performed also on several forms of the protein differing in the number and/or the oxidation state of the bound metal ions and in the presence or absence of peroxide, namely, oxy-[Cu(II)O_2^{2-}Cu(II)], deoxy-[Cu(I)Cu(I)], met-[Cu(II)Cu(II)], half-met-[Cu(I)Cu(II)], half-apo-[Cu(I)–], and apo.

Materials and Methods

Octopus vulgaris Hc was prepared from the hemolymph collected from living animals at the Zoological Station of Napoli (Napoli, Italy) as described by Salvato et al. (1979). Pure preparations of either 50S or 11S *Octopus* Hc were obtained from the native protein as described elsewhere (Salvato et al., 1979; Beltramini et al., 1984b). Half-apo and apo derivatives were prepared according to the method of Beltramini et al. (1984a); half-met- and met-Hc were prepared according to the method of Salvato et al. (1986a,b). Deoxy-Hc was prepared either by addition of 0.01 M sodium sulfite to native Hc in the presence of catalytic amounts of Cu(II) (Ma et al., 1977) or by equilibration of oxy-Hc in N_2 atmosphere. CO–Hc was prepared by adding pure CO gas to deoxy-Hc obtained under N_2 atmosphere in a tonometer equipped with a fluorescence cell. Full conversion to CO–Hc was checked by the constancy of the emission at 545 nm typical of the CO–Hc complex (Finazzi-Agrò et al., 1982). The ANS–Hc complex was prepared from the apo form in 20 mM Tris-HCl buffer, pH 8.8, as described by Ricchelli and Salvato (1979). Chemicals were of the best grade commercially available and were used without further purification.

Protein concentration was measured spectrophotometrically by using the absorption coefficient $\epsilon_{278}^{0.1\%} = 1.43$ in 10 mM Tris-HCl, pH 7.4. Absorption spectra were recorded with a Perkin-Elmer Lambda 5 spectrophotometer.

Steady-State Fluorescence Measurements. Fluorescence spectra were recorded with a Perkin-Elmer MPF4 spectrophotofluorometer equipped with a thermostated cell holder; the "ratio" mode was used to correct for light-source fluctuations. Emission and excitation spectra were corrected for the inner filter or self-absorption effects by the multiplying factor $X = \text{antilog}\,(A_{exc} + A_{em})/2$, where A_{exc} and A_{em} are the absorbances at the excitation and emission wavelengths, respectively.

Relative quantum yields (Q) were measured by comparing the integrated corrected fluorescence emission spectra with those of *N*-acetyltryptophanamide, normalized to the same absorbance at the excitation wavelength. The quantum yield of the standard is 0.13 at 21 °C (Ricchelli et al., 1980).

Singlet–singlet energy transfer from Hc tryptophan residues to the copper peroxide complex or to the active site bound CO and ANS was calculated (Förster, 1959) by the equation

$$R_0 = (9.79 \times 10^3)(Jn^{-4}K^2Q_0)^{1/6} \quad (1)$$

where R_0 (in angstroms) is the critical distance for a 50% probability of energy transfer, n is the refractive index of the medium ($n = 1.33$; Moog et al., 1984), Q_0 is the quantum yield of donor fluorescence in the absence of energy transfer, and K_2 is a factor determined by the mutual orientation in space of the transition dipole moments of donor and acceptor species. In the absence of detailed knowledge about the exact distribution and relative orientations of the individual donors and acceptors, we refer to "an equivalent oscillators model" consisting of a single donor–acceptor pair with parallel orientation, so that $K_2 = 1$, as proposed by Shaklai and Daniel (1970). The quantity

$$J_{AD} = \int_0^\infty F_D(\nu)\epsilon_A(\nu)\nu^{-4}\,d\nu \quad (2)$$

is the overlap integral between $\epsilon_A(\nu)$, the decadic molar absorbance of the acceptor, and $F_D(\nu)$, the donor-corrected emission spectrum on a wavenumber scale normalized to unity (Conrad & Brand, 1968). The Trp emission spectra were corrected by reference to the corrected emission spectrum of indole (Berlman, 1965). The absorption spectra of the acceptors were determined by difference spectroscopy using a solution of either apo-Hc (for ANS–Hc complex) or deoxy-Hc (for CO–Hc complex) as reference. The distance r between the energy donor and acceptor was determined by the expression

$$e = R_0^6/(R_0^6 + r^6) \quad (3)$$

where e is the efficiency of the energy-transfer process. This can be related to the donor quantum yield or fluorescence lifetime by

$$e = 1 - \frac{Q_{D\to A}}{Q_D} \qquad e = 1 - \frac{\tau_{D\to A}}{\tau_D} \quad (4)$$

where $Q_{D\to A}$ (or $\tau_{D\to A}$) and Q_D (or τ_D) are the donor quantum yield (or fluorescence lifetime) in the presence or absence of an acceptor, respectively.

Fluorescence quenching experiments were performed with acrylamide and I^- as external quenchers. When I^- was used, the ionic strength of the solutions was kept constant by addition of suitable amounts of KCl. For double-quenching experiments (Ricchelli & Zatta, 1985; Ricchelli et al., 1986), Hc solutions containing 0.45 M KI were additionally treated with increasing concentrations of acrylamide. The fluorescence quenching data were analyzed according to the Stern–Volmer relationship (Lehrer, 1971)

$$F^0/F = 1 + K_Q[X] \quad (5)$$

where F^0 and F are the fluorescence intensities in the absence and presence of the quencher, respectively, and [X] is the quencher concentration. K_Q is the apparent quenching constant. In the case of heterogeneous emission a modified Stern–Volmer equation can be applied, which, at low quencher concentrations, has the form

$$F^0/(F^0 - F) = (1/[X])(1/\Sigma f_i K_{Q_i}) + \Sigma K_{Q_i}/\Sigma f_i K_{Q_i} \quad (6)$$

Table I: Spectroscopic Properties of Oxy-Hc, CO-Hc, and ANS-Hc

species	donor emission max[a] (nm)	acceptor emission max[b] (nm)	acceptor absorption max (nm)	ϵ acceptor (M^{-1} cm^{-1})	J (M^{-1} cm^{-3})	Q_0[c]	e[d]	R_0 (nm)	r (nm)
O_2^{2-}-Hc	331		348	18000	2.7×10^{-14}	0.040	0.67 (0.2)	2.5	2.2 (3.1)
CO-Hc	331	545	305	2400	9.48×10^{-16}	0.040	0.43	1.5	1.5
ANS-Hc	331	470	350	4900	1.58×10^{-14}	0.049	0.95	2.4	1.5

[a] Excitation wavelength = 295 nm. [b] Excitation wavelength = 295 nm or 305 and 350 nm, respectively, for CO-Hc and ANS-Hc. [c] Q_0 is the quantum yield of the reference system in the absence of energy transfer, namely, deoxy-Hc for O_2^{2-}-Hc and CO-Hc derivatives and apo-Hc for ANS-Hc derivatives, and it is calculated by using *N*-acetyltryptophanamide as reference standard. [d] Calculated from quantum yield measurements (see Materials and Methods). The value in parentheses is calculated from lifetime measurements by using the weighted average of the two values (see Table III).

where $\sum K_{Q_i}$ = intercept/slope can be considered the effective quenching constant $(K_Q)_{eff}$ and $\sum f_i K_{Q_i} / \sum K_{Q_i} = 1/\text{intercept}$ is the effective fractional maximum accessible fluorescence $(f_a)_{eff}$ (Lehrer, 1971).

The contribution of static quenching has been corrected by using the equation (Eftink & Ghiron, 1976)

$$F^0/[F \exp(V[X])] = 1 + K_Q[X] \quad (7)$$

where V is a constant whose value ranges between 0 and 2.5 M^{-1} for several proteins and model compounds (Eftink & Ghiron, 1976). K_Q was determined by assuming the V value that gives a linear F^0/F versus [X] plot.

Time-Resolved Fluorescence Measurements. Fluorescence decays were measured by a single-photon time correlation apparatus. A thyratron-gated flash lamp, filled with deuterium at 0.5 atm, was used for excitation. The repetition frequency of the lamp was adjusted at 40 kHz, with an anode voltage of 5 kV and an electrode gap of 3 mm. The instrumental pulse profile was characterized by a full width at half-maximum of ca. 2.5 ns. A monochromator selected the excitation wavelength at 290 nm. The emission was detected at right angles by using a Philips 56 DUVP photomultiplier. A Balzers K40 interference filter in combination with cutoff at 324 and 305 nm was used to select the emitted light. The excitation profiles were registered at 290 nm by placing an Al reflector in the sample holder. Each signal was collected and stored in 256 channels of a multichannel analyzer and fed into a Cromemco microcomputer.

Decay profiles were analyzed by the method of iterative reconvolution employing a nonlinear least-squares procedure. All the decays could be satisfactorily fitted by a two-exponential decay law. The resulting residuals were regularly distributed along the time axis, and the reduced χ^2 values were ≤ 1.5. The weighted residuals are defined as $R_i = (y_i - f_i)/(f_i)^{1/2}$, where y_i represents the data point and f_i represents the calculated point. The reduced χ^2 value is defined as χ^2/ν, where ν is the number of degrees of freedom ($\simeq$number of points) and $\chi^2 = \sum_i [y_i - f_i)/(f_i)^{1/2}]^2$. Each reported lifetime, τ, was obtained from the average of three measurements, the scatter being <10%. The fractional contribution of each decay component to the total fluorescence (F^{fr}) was calculated as

$$F_1^{fr} = \frac{A_1\tau_1}{A_1\tau_1 + A_2\tau_2}; \qquad F_2^{fr} = 1 - F_1^{fr} \quad (8)$$

Further details on the apparatus and the treatment of the data are reported elsewhere (Gardini et al., 1980).

Results

Energy-Transfer Studies. The absorption and emission properties of ANS and CO derivatives of *Octopus* Hc are reported in Table I, together with those characteristic of the oxy form. CO- and ANS-Hc complexes show the fluorescence emission from both Trp residues and the external ligand. No fluorescence is emitted by the $Cu_2O_2^{2-}$.

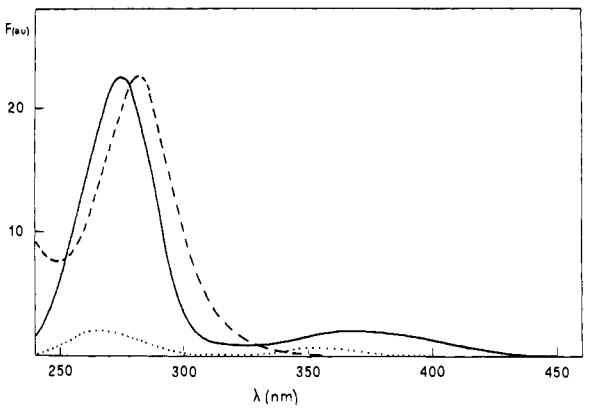

FIGURE 1: Fluorescence excitation spectra of ANS-Hc (solid line, λ_{em} = 470 nm), of CO-Hc (dashed line, λ_{em} = 545 nm), and of free ANS in buffer (dotted line, λ_{em} = 470 nm). ANS and ANS-Hc were dissolved in 20 mM Tris-HCl buffer, pH 8.8, and CO-Hc was dissolved in 10 mM Tris-HCl buffer, pH 8.0, at T = 21 °C. Fluorescence intensity is in arbitrary units.

The fluorescence excitation spectra of ANS-Hc and CO-Hc (Figure 1), recorded at the emission maxima of the external ligand (470 and 545 nm, respectively), show a band in the 240-300-nm spectral region that is typical for Trp absorption. Ligand-free Hc does not show any excitation spectrum around 280 nm when the same emission wavelengths are used. The ANS-Hc excitation spectrum is blue-shifted compared to CO-Hc because of the contribution of the free ANS, whose excitation maximum is at 265 nm.

From the degree of quenching of intrinsic fluorescence upon binding of the external ligand, energy-transfer efficiencies of 0.43 and 0.95 are calculated, respectively, for CO-Hc and ANS-Hc derivatives (Table I). In the case of oxy-Hc, an efficiency of 0.67 for the hypothetical energy-transfer process from Trp residues to the copper-oxygen band can be calculated on the basis of the difference in fluorescence quantum yields between deoxy and oxy derivatives. However, a much smaller value of e = 0.20 is obtained by using the fluorescence lifetimes.

In the calculation of overlap integrals, the reference system in the absence of energy transfer is apo-Hc for the ANS-Hc derivative and deoxy-Hc for CO-Hc and oxy-Hc complexes. As shown in Table I, deoxy-Hc displays a fluorescence quantum yield Q = 0.04, higher than that previously reported (0.03; Ricchelli, 1982). This is due to the absence in the present preparations of O_2, which is known to be an efficient quencher of Trp fluorescence (Lakowicz & Weber, 1973). The interference of dissolved O_2 must be taken into account when Q of Hc derivatives is compared with that of the deoxy form. The J value obtained with the CO-Hc complex is ca. 2 orders of magnitude smaller than those of ANS-Hc and oxy-Hc,

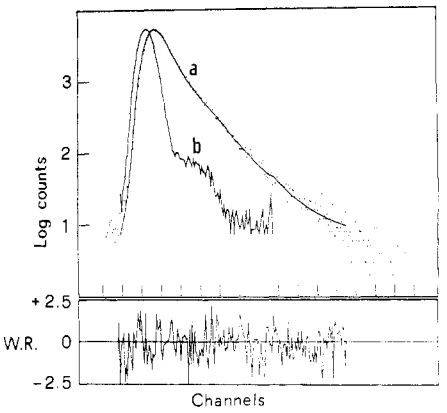

FIGURE 2: Fluorescence decay profile of apo-Hc under an excitation wavelength of 290 nm. Apo-Hc, in 11S aggregation state, was dissolved in 10 mM Tris-HCl buffer, pH 8.5, after dialysis against 10 mM EDTA to remove Ca^{2+}. Top panel: (a) fitting by two-exponential analysis of decay curve; (b) excitation light profile. Bottom panel: distribution of weighted residuals (W.R.). For details see Materials and Methods.

Table II: Decay Parameters for Hc Derivatives in 50S Aggregation State[a]

sample	τ_1 (ns)	$A_1{}^b$ (%)	$F_1{}^{fr\,c}$	τ_2 (ns)	$A_2{}^b$ (%)	$F_2{}^{fr\,c}$
oxy-Hc	0.5	87	0.5	3.4	13	0.5
half-met-Hc	0.6	92	0.65	3.7	8	0.35
met-Hc	0.54	89	0.54	3.7	11	0.46
deoxy-Hc	0.90	74	0.43	3.4	26	0.57
apo-Hc	0.80	87	0.58	3.9	13	0.42

[a] Experiments performed in 0.01 M Tris-HCl, pH 8.0, in the presence of 20 mM $CaCl_2$. [b] Relative weights of decay of the different lifetimes. [c] Fractional contribution of the different decay components to the total fluorescence calculated from the relationship $F_i^{fr} \propto A_i\tau_i$.

Table III: Decay Parameters and Relative Quantum Yields for Hc Derivatives in 11S Aggregation State[a]

sample	τ_1 (ns)	$A_1{}^b$ (%)	$F_1{}^{fr\,b}$	τ_2 (ns)	$A_2{}^b$ (%)	$F_2{}^{fr\,b}$	$Q/Q_{oxy}{}^c$
oxy-Hc	1.10	89	0.64	5.1	11	0.36	1.0
half-met-Hc	1.16	94	0.77	5.4	6	0.23	2.0
met-Hc	1.20	87	0.65	4.3	13	0.35	2.3
deoxy-Hc	1.80	75	0.48	5.9	25	0.52	4.0[d]
half-apo-Hc	2.10	79	0.58	5.7	21	0.42	5.0
apo-Hc	2.10	80	0.60	5.5	20	0.40	5.1

[a] Experiments performed in 0.01 M Tris-HCl, pH 8.5, after dialysis of the samples against 10 mM EDTA. [b] See footnotes to Table II. [c] Quantum yields of the derivatives referred to that of oxy-Hc (see Table I). [d] Quantum yield in the absence of O_2.

owing to both the lower extinction coefficient and the blue-shifted position of the maximum of the corresponding absorption band.

Using the parameters of Table I, we calculate a donor–acceptor distance r of 1.5 nm in the case of both CO–Hc and ANS–Hc. Much higher values are obtained for oxy-Hc (2.2 or 3.1 nm).

Time-Resolved Fluorescence Studies. The decay profiles of the first excited singlet state of Trp residues in Hc derivatives are satisfactorily fitted by two-exponential analysis, in agreement with the heterogeneous distribution of the fluorophores. In Figure 2 is reported a typical profile of Hc fluorescence decay with the two-exponential fitting. The lifetime (τ), the relative weight (A) of the decay of the two components, and the fractional contribution (F^{fr}) of each component to the total fluorescence are reported in Tables II and III for Hc derivatives in 50S and 11S aggregation states, respectively. The quantum yield of each Hc derivative, relative

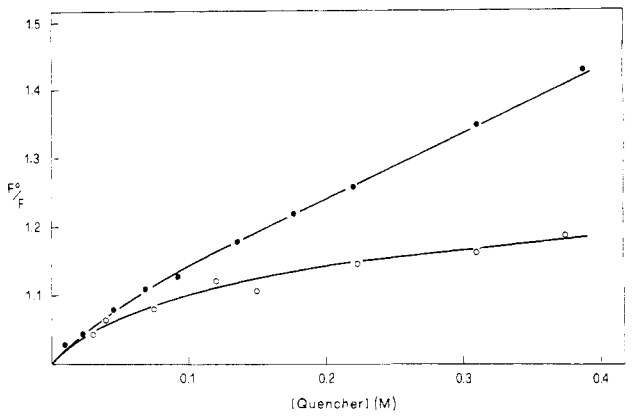

FIGURE 3: Quenching of Hc fluorescence: Stern–Volmer plots describing the quenching of apo-Hc (11S) fluorescence by acrylamide (●) and iodide (○). The plots were obtained by applying eq 5. Apo-Hc was dissolved in 10 mM Tris-HCl buffer, pH 8.5.

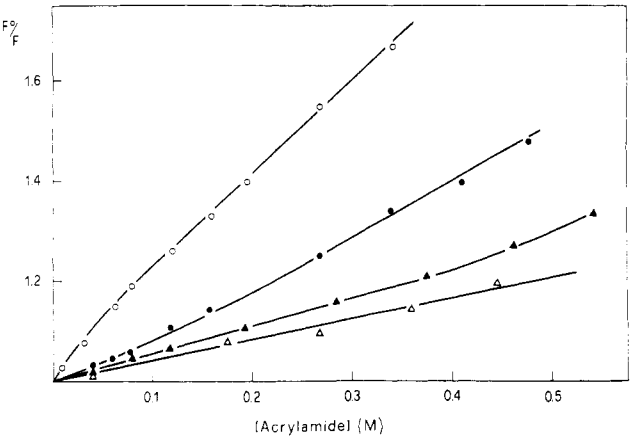

FIGURE 4: Double quenching of Hc fluorescence: Stern–Volmer plots (eq 5) describing the acrylamide quenching of native Hc (●), apo- and half-apo-Hc (○), met-Hc (▲), and half-met-Hc (△) fluorescence in the presence of 0.45 M KI. All samples were dissolved in 10 mM Tris-HCl buffer, pH 8.5.

to that of oxy-Hc, is also reported for 11S Hc (see Table III).

A characteristic feature of the data of Tables II and III is that the short-lived component is mostly responsible for the observed decay. Furthermore, aggregation of Hc to 50S leads to a shortening of the lifetimes of both components.

Modification of the oxidation state of the copper or removal of the metal brings about a marked change of the fluorescence quantum yields.

Fluorescence Quenching Studies. Fluorescence quenching experiments were performed on Hc in aggregation state 11S at pH 8.5; these conditions are the most appropriate for discriminating between the different classes of fluorophores in *Octopus* Hc by means of acrylamide quenching (Ricchelli et al., 1984).

For all Hc derivatives, the Stern–Volmer plots show a considerable decrease in slope at increasing quencher concentrations, indicative of heterogeneous distribution of fluorophores. As an example, in Figure 3 the Stern–Volmer plots describing the quenching of apo-Hc fluorescence by either acrylamide or iodide are shown. After treatment of the quenching data according to the modified Stern–Volmer equation (eq 6) (data not shown), the same fraction (f_a = 0.38 for apo-Hc) of accessible fluorescence is calculated with both quenchers. The Stern–Volmer constant associated with this fraction is 5.7 M^{-1} for acrylamide quenching. For the other derivatives, f_a, calculated from either acrylamide or iodide quenching, ranges between 0.30 and 0.38.

Table IV: Acrylamide Fluorescence Quenching Parameters of Hc Derivatives in 11S Aggregation State (in 0.01 M Tris-HCl, pH 8.5) in the Presence of 0.45 M I^-

sample	f_a	V (M^{-1})	K_Q (M^{-1})
oxy-Hc	1.0	0.25	0.60
half-met-Hc	1.0	0.01	0.45
met-Hc	1.0	0.06	0.50
half-apo-Hc	0.75	0	4.13
apo-Hc	0.70	0	4.50

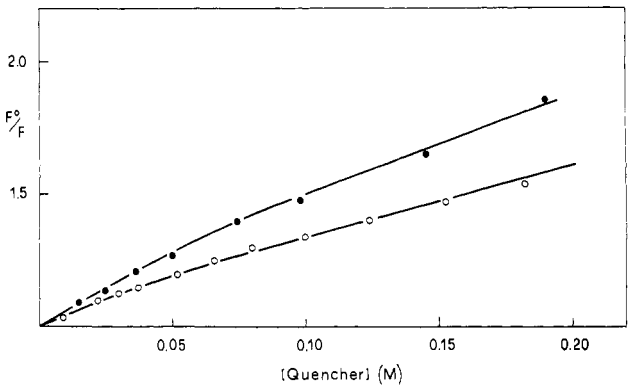

FIGURE 5: Quenching of Hc fluorescence: Stern–Volmer plots (eq 5) describing the quenching of deoxy-Hc fluorescence by acrylamide (●) and iodide (○). Deoxy-Hc was dissolved in 10 mM Tris-HCl buffer, pH 8.5.

Stern–Volmer plots obtained from the double-quenching experiments, in the simultaneous presence of both I^- and acrylamide, are shown in Figure 4. A downward curvature of the plots is observed for half-apo- and apo-Hc, whereas the upward curvature of the plots obtained with oxy-, half-met-, and met-Hc indicates the occurrence of static quenching. In Table IV, the results of the double-quenching experiments, after correction for static quenching, are summarized for all Hc derivatives.

The Stern–Volmer plots obtained from the data of acrylamide and iodide quenching for deoxy-Hc are shown in Figure 5. From the plot modified according to eq 6 (data not shown) it is calculated that about 57–60% of fluorescence is affected by both quenchers with a K_Q value of 8.0 M^{-1} for acrylamide quenching.

Discussion

The Trp active site average distance in *Octopus* Hc was calculated according to the Förster equation with a number of energy acceptors, such as the copper–peroxide complex and carbon monoxide and ANS specifically bound to the active site in a 1:1 ratio (Alben et al., 1970; Yen Fager & Alben, 1972; Finazzi-Agrò et al., 1982; Ricchelli & Salvato, 1979).

The existence of a radiationless energy-transfer process, which is the basis for this calculation, is well demonstrated for ANS–Hc and CO–Hc by the appearance of the Trp excitation band when the emission wavelengths are set to the maxima of the added ligands. There is also a concomitant decrease of the protein intrinsic fluorescence intensity (at 331 nm). Precise evidence for energy transfer from the excited Trp to the copper–peroxide complex, on the contrary, is lacking in oxy-Hc as there is no emission associated with the absorption band arising from oxygen binding; on the other hand, evidence for such a process was proposed by indirect measurements (Shaklai & Daniel, 1970, 1972). We observe that a large discrepancy exists between the values of the Trp active site distance calculated for either ANS- or CO–Hc and oxy-Hc. However, a substantial identity is found in the case of ANS–Hc and CO-Hc.

Time-resolved and fluorescence quenching experiments, performed on a number of Hc derivatives, allow us to explain this discrepancy.

Acrylamide quenching data indicate that in all derivatives 30–38% of fluorescence is associated with surface residues even if the value of the quenching constant (K_Q = 5.7 M^{-1} for apo-Hc) is lower than those typical for fully exposed Trp in proteins (K_Q = 9–12 M^{-1}; Kirby & Steiner, 1970). However, previous results (Ricchelli et al., 1984) showed that in *Octopus* Hc surface tryptophans lie in the subunit interfaces, being partially shielded by the protein quaternary structure. Moreover, the same fraction of fluorescence is selectively quenched by I^-, which is known to preferentially interact with external fluorophores, its large hydration sphere precluding penetration to the protein matrix. It is noteworthy that the contribution of the exposed tryptophans in all Hc derivatives, deduced from fluorescence quenching experiments, corresponds rather well to the percentage of the total fluorescence attributable to the long-lived component obtained from time-resolved experiments (see Table III). In addition, in the presence of I^- we observed a selective shortening of the longer lifetime in all Hc derivatives (data not shown).

Taken together, these findings allow us to assign a τ on the order of 4.3–5.9 ns to the class of exposed tryptophans. The shortening of this lifetime in the 50S aggregation state (Table II) is attributable to the strong influence of quaternary structure, which increases Trp burial and normalizes the environments (Ricchelli et al., 1984).

The selective effect of I^- on surface residues allows us to eliminate the contribution of this Trp class to the overall fluorescence; hence, the residual emission can be further discriminated by acrylamide. As shown in Table IV, only one class of Trp (f_a = 1.0) is still present in oxy-, half-met-, and met-Hc, as also deduced from the occurrence of static quenching (Figure 4; Eftink & Ghiron, 1976). The very low K_Q value (K_Q = 0.45–0.6 M^{-1}) is indicative of a deep burial of the fluorophores (Kirby & Steiner, 1970). These findings confirm the presence of only two classes of Trp in *Octopus* oxy-Hc; in addition, we can associate the short-lived τ of 1.1 ns with the class of deeply buried Trp. The close similarity of f_a, K_Q, and τ values of oxy-Hc with those of the half-met and met forms strongly supports the proposition that the Trp residues' distribution and the conformational properties of their microenvironment are not changed in the latter derivatives.

In apo- and half-apo-Hc heterogeneous emission is still present after I^- quenching (Figure 4). This is consistent with the demasking of Trp near the active site, as a consequence of the removal of one or both copper ions. The contribution of these fluorophores to the residual fluorescence is about 70–75% (42–44% of the overall fluorescence). It is supposed that the contribution of buried Trp to the fluorescence does not change in half-apo- and apo-Hc as only limited conformational changes occur after copper removal (Tamburro et al., 1976); on these bases, it is reasonable to assign the τ value of 2.1 ns to Trp near the active site, taking also into account that these tryptophans are mostly responsible for the fluorescence of these derivatives. The double-exponential analysis of the decay profiles actually underestimated this value, although the contribution of the buried Trp to the overall fluorescence in half-apo- and apo-Hc does not exceed 12–18%.

Acrylamide quenching and time-resolved experiments indicate that Trp residues are more accessible in deoxy-Hc (about 60% of fluorescence with K_Q = 8.0 M^{-1} and τ = 5.9 ns). This is also the conclusion from I^- quenching experiments: the considerable slope of the quenching curve (Figure 5) at

high I^- concentrations suggests that I^- does not preferentially interact with external fluorophores. Thus, the deoxy-Hc molecule is not as compact as either the native Hc or the apo-Hc.

From the comparison of the lifetime values of deoxy-Hc with that of apo-Hc (Table III), one should expect a higher quantum yield for the former derivative, in contrast with the experimental finding. To account for this discrepancy, we suggest that not all residues which absorb in deoxy-Hc contribute to the emission. As previously proposed by Ricchelli et al. (1983), the heavy atom effect, exerted by bound copper, can provide an efficient quenching mechanism. Since this is a short-range process (Kasha, 1952), it must extinguish selectively the emission of one or more fluorophores in close proximity to the active site. Moreover, time-resolved emission experiments confirm that only the copper which is first removed from the active site is responsible for the heavy atom effect. Indeed, half-apo-Hc (Table III) shows no difference in Q, τ, or A if compared with apo-Hc.

The further quenching of Q observed in half-met- and met-Hc can be attributed to the "paramagnetic ion" effect due to Cu(II). This completely abolishes the residual fluorescence of the Trp class near the active site since the component with $\tau = 2.1$ ns is not present in these derivatives. Accordingly, the fluorescence quenching in half-met- and met-Hc derivatives accounts for about 45% of the deoxy-Hc fluorescence, which corresponds to the contribution to the overall fluorescence of the Trp residues near the active site. Some influence of the paramagnetic ion effect may occur also on external Trp residues, as deduced from the shortening of the long-lived component of the decay in met-Hc (Table III).

It is clear from these findings that both heavy atom and paramagnetic ion effects can fully account for the fluorescence quenching of the Trp class near the active site in oxy-Hc. Thus, an energy-transfer process from these residues to the copper–peroxide complex is unlikely.

The occurrence of such a process from the other two classes of Trp seems also unlikely on the basis of the following considerations. The efficiency of the energy-transfer mechanism is correctly evaluated if the typical protein conformation is preserved in the reference system. As shown in this study, met-Hc and oxy-Hc display very similar conformational properties; a different situation occurs for deoxy-Hc, which was chosen as the reference system in the previous calculations of Trp active site distance. Thus, when met-Hc is taken as the reference system, the efficiency of the hypothetical energy-transfer process is 0.565 when calculated from the quantum yields but only 0.04 when calculated from the lifetimes. If the energy transfer was the main quenching mechanism in oxy-Hc, a good coincidence between the two values should be observed (Haugland et al., 1969). A possible explanation for the discrepancy could be the occurrence of a static quenching effect by bound oxygen on some neighboring Trp. In this case, a decrease of Trp fluorescence quantum yield in oxy-Hc without a corresponding decrease of lifetime (see Table III) is expected (Teale & Badley, 1970; Lakowicz & Weber, 1973).

In conclusion, the application of Förster's theory in calculating Trp active site average distance in oxy-Hc is not justified. The shorter values obtained in this work (1.5 nm) by using CO- and ANS–Hc are more plausible than those reported by other authors: since the quenching effect of bound cupric ions is absent in these derivatives, the average distance calculated by us gives weight also to the contribution of the class of Trp near the active site, which is mostly responsible for the fluorescence emission in Hc.

The interpretation given herein of the fluorescence quenching mechanisms in Hc allows us also to explain some recent findings observed in *Neurospora crassa* tyrosinase. By application of Förster's theory for an equivalent oscillators system, an average Trp active site interaction distance of 2.7 nm has been calculated. However, the same distance calculated in CO–tyrosinase gives a much smaller value of 1.2 nm (Beltramini & Lerch, 1984). It is known that tyrosinase and Hc, though performing different biological functions, contain very similar copper active sites. It is likely, therefore, that heavy atom and paramagentic ion effects can fully account for the fluorescence quenching observed also in native tyrosinase.

ACKNOWLEDGMENTS

We thank Prof. J. W. Longworth (Illinois Institute of Technology, Chicago, IL) for helpful discussion and criticism and A. Cervellin for his skillful technical assistance.

Registry No. Cu, 7440-50-8; I^-, 20461-54-5; Trp, 73-22-3; acrylamide, 79-06-1.

REFERENCES

Alben, J. O., Yen, L., & Farrier, N. J. (1970) *J. Am. Chem. Soc. 92*, 4475–4476.

Bannister, W. H., & Wood, E. J. (1971) *Comp. Biochem. Physiol., B: Comp. Biochem. 40B*, 7–18.

Beltramini, M., & Lerch, K. (1983) in *The Coordination Chemistry of Metallo-enzymes* (Bertini, I., Drago, R. S., & Luchinat, C., Eds.) pp 235–239, D. Riedel, Basel.

Beltramini, M., Ricchelli, F., Piazzesi, A., Barel, A., & Salvato, B. (1984a) *Biochem. J. 221*, 911–914.

Beltramini, M., Ricchelli, F., & Salvato, B. (1984b) *Inorg. Chim. Acta 92*, 209–217.

Beltramini, M., Ricchelli, F., Tallandini, L., & Salvato, B. (1984c) *Inorg. Chim. Acta 92*, 219–227.

Beltramini, M., Piazzesi, A., Alviggi, M., Ricchelli, F., & Salvato, B. (1986) in *Invertebrate Oxygen Carriers* (Linzen, B., Ed.) pp 429–433, Springer, Berlin.

Berlman, I. B. (1965) in *Handbook of Fluorescence Spectra of Aromatic Molecules* (Berlman, I. B., Ed.) p 101, Academic, New York.

Brown, J. M., Powers, L., Kincaid, B., Larrabee, J. A., & Spiro, T. G. (1980) *J. Am. Chem. Soc. 102*, 4210–4216.

Conrad, R., & Brand, L. (1968) *Biochemistry 7*, 777–787.

Cox, J. A., & Elliott, F. G. (1974) *Biochim. Biophys. Acta 371*, 392–401.

Eftink, M. R., & Ghiron, C. A. (1976) *J. Phys. Chem. 80*, 486–493.

Ellerton, H. D., Ellerton, N. F., & Robinson, H. A. (1983) *Prog. Biophys. Mol. Biol. 41*, 143–248.

Finazzi-Agrò, A., Zolla, L., Flamigni, L., Kuiper, H. A., & Brunori, M. (1982) *Biochemistry 21*, 415–418.

Förster, T. (1959) *Discuss. Faraday Soc. 27*, 7–17.

Gardini, E., Dellonte, S., Flamigni, L., & Barigelletti, F. (1980) *Gazz. Chim. Ital. 110*, 533–537.

Haugland, R. P., Yguerabide, J., & Stryer, L. (1969) *Proc. Natl. Acad. Sci. U.S.A. 63*, 23–30.

Himmelwright, R. S., Eickman, N. C., Lu Bien, C. D., & Solomon, E. I. (1979) *J. Am. Chem. Soc. 101*, 1576–1586.

Jori, G., Ricchelli, F., Salvato, B., Tallandini, L., & Cannistraro, S. (1981) in *Invertebrate Oxygen-Binding Proteins* (Lamy, J., & Lamy, J., Eds.) pp 621–632, Marcel Dekker, New York.

Kasha, M. (1952) *J. Chem. Phys. 20*, 71–75.

Kirby, E. P., & Steiner, R. F. (1970) *J. Biol. Chem. 245*, 6300–6306.

Klarman, A., Shaklai, N., & Daniel, E. (1977) *Biochim. Biophys. Acta 490*, 322–330.
Lakowicz, J. R., & Weber, G. (1973) *Biochemistry 12*, 4161–4170.
Lehrer, S. S. (1971) *Biochemistry 10*, 3254–3263.
Linzen, B., Soeter, N. M., Riggs, A. F., Schneider, H. J., Schartau, W., Moore, M. D., Yokota, E., Behrens, P. Q., Nakashima, H., Takagi, T., Nemoto, T., Vereijken, J. M., Bak, H. J., Beintema, J. J., Volbeda, A., Gaykema, W. P. J., & Hol, W. G. J. (1985) *Science (Washington, D.C.) 229*, 519–529.
Ma, J. K. H., Luzzi, L. A., Ma, T. Y. C., & Li, N. C. (1977) *J. Pharm. Sci. 66*, 1684–1687.
Moog, R. S., Kuki, A., Fayer, M. D., & Boxer, S. G. (1984) *Biochemistry 23*, 1564–1571.
Ricchelli, F. (1982) *Med. Biol. Environ, 10*, 327–331.
Ricchelli, F., & Salvato, B. (1979) *Eur. J. Biochem. 94*, 199–205.
Ricchelli, F., & Zatta, P. (1985) *Med. Biol. Environ. 13*, 105–108.
Ricchelli, F., Salvato, B., Filippi, B., & Jori, G. (1980) *Arch. Biochem. Biophys. 202*, 277–288.
Ricchelli, F., Tealdo, E., & Salvato, B. (1983) *Life Chem. Rep., Suppl. Ser. 1*, 301–304.
Ricchelli, F., Jori, G., Tallandini, L., Zatta, P., Beltramini, M., & Salvato, B. (1984) *Arch. Biochem. Biophys. 235*, 461–469.
Ricchelli, F., Filippi, B., Gobbo, S., Simoni, E., Tallandini, L., & Zatta, P. (1986) in *Invertebrate Oxygen Carriers* (Linzen, B., Ed.) pp 235–239, Springer, Berlin.
Salvato, B., & Zatta, P. (1977) in *Structure and Function of Hemocyanin* (Bannister, J. V., Ed.) pp 245–252, Springer, Berlin.
Salvato, B., Ghiretti-Magaldi, A., & Ghiretti, F. (1979) *Biochemistry 18*, 27–37.
Salvato, B., Giacometti, G. M., Alviggi, M., & Giacometti, G. (1986a) in *Invertebrate Oxygen Carriers* (Linzen, B., Ed.) pp 457–462, Springer, Berlin.
Salvato, B., Giacometti, G. M., Alviggi, M., & Giacometti, G. (1986b) in *Invertebrate Oxygen Carriers* (Linzen, B., Ed.) pp 453–456, Springer, Berlin.
Shakali, N., & Daniel, E. (1970) *Biochemistry 9*, 564–568.
Shaklai, N., & Daniel, E. (1972) *Biochemistry 11*, 2199–2203.
Shaklai, N., Gafni, A., & Daniel, E. (1978) *Biochemistry 17*, 4438–4442.
Symons, M. C. R., & Petersen, R. L. (1978) *Biochim. Biophys. Acta 535*, 247–252.
Tamburro, A. M., Salvato, B., & Zatta, P. (1976) *Comp. Biochem. Physiol., B: Comp. Biochem. 55B*, 347–356.
Teale, F. W. J., & Badley, R. A. (1970) *Biochem. J. 116*, 341.
Yen Fager, L., & Alben, J. O. (1972) *Biochemistry 11*, 4786–4792.
Yokota, E., Moore, M. D., Behrens, P. Q., & Riggs, A. F. (1983) *Life Chem. Rep. Suppl. Ser. 1*, 75–80.

Proton NMR Characterization of Isomeric Sulfmyoglobins: Preparation, Interconversion, Reactivity Patterns, and Structural Features†

Mariann J. Chatfield, Gerd N. La Mar,* and Robert J. Kauten
Department of Chemistry, University of California, Davis, California 95616
Received April 1, 1987; Revised Manuscript Received May 20, 1987

ABSTRACT: The preparations of sulfmyoglobin (sulf-Mb) by standard procedures have been found heterogeneous by ^{1}H NMR spectroscopy. Presented here are the results of a comprehensive study of the factors that influence the selection among the three dominant isomeric forms of sperm whale sulf-Mb and their resulting detailed optical and ^{1}H NMR properties as related to their detectability and structural properties of the heme pocket. A single isomer is formed initially in the deoxy state; further treatment in any desired oxidation/ligation state can yield two other major isomers. Acid catalysis and chromatography facilitate formation of a second isomer, particularly in the high-spin state. At neutral pH, a third isomer is formed by a first-order process. The processes that alter oxidation/ligation state are found to be reversible and are judged to affect only the metal center, but the three isomeric sulf-Mbs are found to exhibit significantly different ligand affinity and chemical stability. The present results allow, for the first time, a rational approach for preparing a given isomeric sulf-Mb in an optimally pure state for subsequent characterization by other techniques. While optical spectroscopy can distinguish the alkaline forms, only ^{1}H NMR clearly distinguishes all three ferric isomers. The ring current shifts in the carbonyl complexes of reduced sulf-Mb complexes support saturation for a pyrrole in each isomer. The hyperfine shift patterns in the various oxidation/spin states of sulf-Mbs indicate relatively small structural alteration, and the proximal and distal sides of the heme suggest that peripheral electronic effects are responsible for the differentially reduced ligand affinities for the three isomeric sulf-Mbs. The first ^{1}H NMR spectra of sulfhemoglobins are presented, which indicate a structure similar to that of the initially formed sulf-Mb isomer but also suggest the presence of a similar molecular heterogeneity as found for sulf-Mb, albeit to a smaller extent.

Sulfhemoglobin (sulf-Hb)[1] is a green heme protein that is physiologically inactive (Park & Nagel, 1984). Since its discovery (Hoppe-Seyler, 1866), this modified hemoglobin and an analogous complex of myoglobin, sulf-Mb, have undergone a variety of studies designed to determine the structural al-

† This work was supported by a grant from the National Institutes of Health (GM-26226).
* Author to whom correspondence should be addressed.

[1] Abbreviations: sulf-Hb, sulfhemoglobin; sulf-Mb, sulfmyoglobin; S_AMb, S_BMb, and S_CMb, isomeric forms of sulfmyoglobin; Mb, myoglobin; Hb, hemoglobin.

0006-2960/87/0426-6939$01.50/0